PROCEEDINGS of the
23rd International Congress on Acoustics

9 to 13 September 2019 in Aachen, Germany

Comparison of ASJ RTN-Model 2013 and the Harmonoise engineering model under thick barrier configurations

Takuya OSHIMA[1]; Azusa HOSHIKAWA[2]; Yumi KUROSAKA[2]

[1] Faculty of Engineering, Niigata University, Japan

[2] Graduate School of Science and Technology, Niigata University, Japan

ABSTRACT

Engineering models for environmental noise are developed in many countries under different backgrounds. Such differences make each model have different characteristics. In European countries, comparative studies have been carried out to illustrate the characteristics of models such as Nord2000, Harmonoise and CNOSSOS-EU. However, comparison of the Japanese road traffic noise model, ASJ RTN-Model 2013, to another model has seldom been made. This is probably because the ASJ model uses A-weighted levels throughout the calculation process, unlike European models that use either octave-band or one-third-octave-band levels. In this study, a methodology to derive consistent quantities between the ASJ model and the European Harmonoise model is established. The methodology is applied to thick barrier test cases that are included in a Harmonoise deliverable. At the same time, finite-difference time-domain simulations are carried out to obtain reference solutions. A-weighted source power levels between the two models are found to be larger for the light vehicle of the ASJ model. Comparison between each model and the reference solutions weighted by each source spectrum agree well for both models. The final A-weighted levels obtained by both models agree within a 2 dB difference.

Keywords: Source power spectrum, Source directivity, Diffraction model

1. INTRODUCTION

Engineering models for environmental noise have been developed in many countries under different backgrounds. Such differences make each model have different characteristics. In European countries, comparative studies have been carried out in open literature to illustrate the characteristics of models such as Nord2000 (1), Harmonoise (2) and CNOSSOS-EU (3). By taking various forms of critical reviews (4, 5) and demonstrative approaches (6, 7, 8, 9), those studies provide insights about the direction towards which a new model should be developed, and thorough validations of a newly developed model. In Japan, there has been revisions of a road traffic noise model since 1975, called ASJ Road Traffic Noise (ASJ-RTN) Model, developed by the Acoustical Society of Japan. Since 1993, the ASJ model has been revised in a cycle of 5 years. However, in spite of such a long history, the characteristics of the ASJ models in comparison with other models have seldom been discussed in open literature. One of the probable reasons is that the ASJ models use A-weighted overall levels throughout the calculation process, unlike other models (in particular the European models) that use either octave-band or one-third-octave-band levels.

In this study, the second latest revision of the ASJ model, ASJ RTN-Model 2013 (10) (referred to as the ASJ model hereafter), is compared with the European Harmonoise engineering model (referred to as the Harmonoise model), which is the predecessor of the current CNOSSOS-EU model, under a simple configuration of a thick barrier along a straight road. The 2013 version of the ASJ model is used because the 2018 version was not yet available at the time when the main part of this study was conducted. The Harmonoise model is chosen because there are many open publications that discuss the development process, details, validation, and test cases of the model. A methodology to derive consistent quantities between the ASJ model and the Harmonoise model, such as the single-vehicle A-weighted power level, is established to make strict comparisons between the two models. The methodology is applied to thick barrier test cases that are included in a Harmonoise deliverable. At

[1] oshima@eng.niigata-u.ac.jp

the same time, finite-difference time-domain simulations are carried out to obtain reference solutions. Then, comparisons of the characteristics of source power modeling, attenuation by diffraction and final predicted A-weighted equivalent sound pressure level are made.

2. OUTLINES OF THE MODELS

Outlines of the models and a methodology to derive consistent quantities between both models are briefly described in this section. The comparisons are made in A-weighted overall levels, as the A-weighted level can be derived from octave-band levels but the opposite is not possible. Thus, as stated later, several steps are added to the calculation procedure of the Harmonoise model to obtain the A-weighted overall levels.

2.1 The ASJ Model

A diagram of a part of the calculation procedure of the ASJ model relevant to this study is shown in Figure 1. First, a source and receiver configuration is given as input. The source road is divided into segments, and a point source i is set at the middle of each segment. The A-weighted source power level of source point i, $L_{WA,i}$, is calculated from the running mode of vehicles, running speed V, and the source directivity ΔL_{dir} for each vehicle category shown in Table 1. Then, the total attenuation $\Delta A_{\mathrm{A},i}$ of the geometric attenuation and the attenuation by diffraction owing to the thick barrier is calculated. The A-weighted sound pressure level (SPL) by source i, $L_{\mathrm{A},i}$, is calculated as follows.

$$L_{\mathrm{A},i} = L_{WA,i} - \Delta A_{\mathrm{A},i} \tag{1}$$

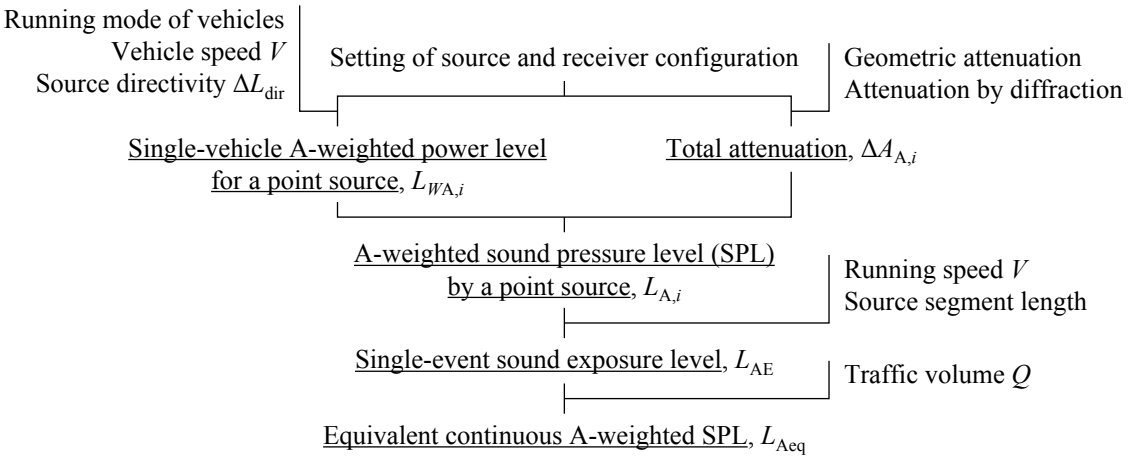

Figure 1 – Calculation procedure of the ASJ model. Underlined variables are calculated ones whereas non-underlined variables are given as input

Table 1 – Vehicle categories

Model	ASJ		Harmonoise
	Two-category	Four-category	
Category	Heavy	Large-sized Medium-sized	Heavy Medium heavy
	Light	Small-sized Passenger	Light
	–		Other heavy
	Motorcycles		Two-wheelers

After calculating $L_{\mathrm{A},i}$ for all point sources, the single-event sound exposure level, L_{AE} by a single vehicle pass-by along the source road is calculated using $L_{\mathrm{A},i}$ for all point sources, the vehicle speed V and the source segment length. Finally, the equivalent continuous A-weighted SPL, L_{Aeq}, is calculated using L_{AE} and the traffic volume Q.

2.2 The Harmonoise Model

A diagram of a part of the calculation procedure of the Harmonoise model relevant to this study and additional steps to obtain consistent quantities with the ASJ model is shown in Figure 2. First, a source and receiver configuration is given as input. The source road is divided into segments and two subsources, each of which is at a height h_s above the ground, are set at the middle of each segment i. The height of one of the two subsources is h_s = 0.01 m and another is either 0.30 m for a light vehicle or 0.75 m for a medium-heavy and a heavy vehicle. The source power level for a single-vehicle subsource, $L'_{W,i,hs}$, is calculated from the vehicle speed V, the source directivity C_{dir}. Calculation of the total power level for a subsource, $L_{W,i,hs}$, follows by using $L'_{W,i,hs}$, the vehicle speed V, the traffic volume Q and the segment length. Then, the total attenuation $\Delta A_{\mathrm{H},i,hs}$ is calculated from the geometric attenuation and the excess attenuation including attenuation by diffraction and ground. The one-third-octave-band SPL for a subsource, $L_{\mathrm{eq1h},i,hs}$, is calculated as

$$L_{\mathrm{eq1h},i,hs} = L_{W,i,hs} - \Delta A_{\mathrm{H},i,hs} \tag{2}$$

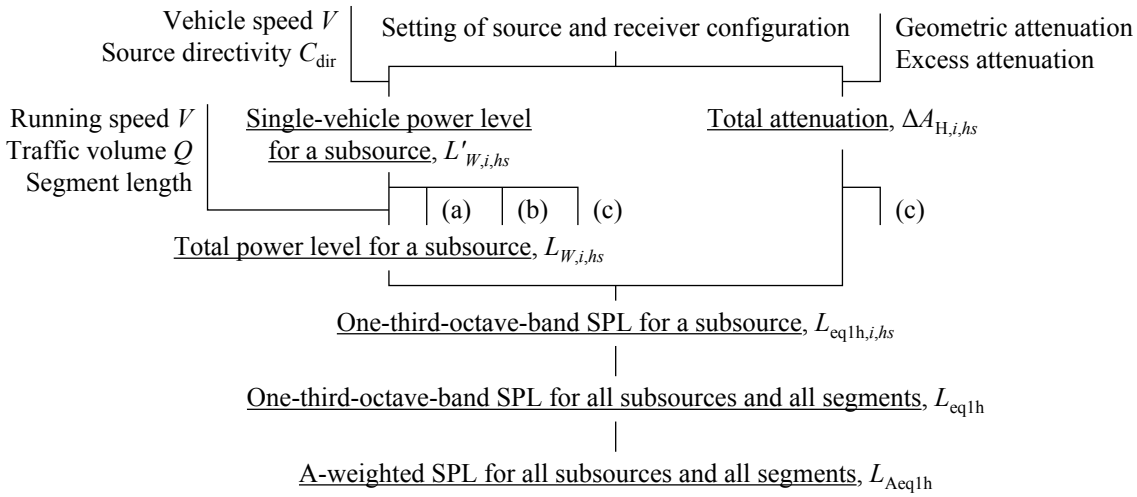

(a) Single-vehicle A-weighted power level for all subsources in source point i, $L_{W\mathrm{A,HN},i}$

(b) A-weighted source directivity, C_{dirA}

(c) A-weighted single-vehicle SPL for all subsources in source point i, $L_{\mathrm{A,HN},i}$

Figure 2 – Calculation procedure of the Harmonoise model. Underlined variables are calculated ones whereas non-underlined variables are given as input

The one-third-octave-band SPL for all subsources and all segments, L_{eq1h}, is calculated by incoherent summation of $L_{\mathrm{eq1h},i,hs}$ over all subsources and all segments. Finally, the A-weighted SPL for all subsources and all segments, L_{Aeq1h}, is computed by summation of L_{eq1h} with A-weighting correction added over all bands.

The excess attenuation $\Delta A_{\mathrm{H},i,hs}$ is calculated using the official Harmonoise point-to-point (P2P) library (11) version 2.022.

2.3 Additional Steps for Obtaining Consistent Quantities between the Models

The vehicle categories defined in each model are associated as shown in Table 1. The large-sized and medium-sized vehicles in four-category classification in the ASJ model are associated with the heavy and medium-heavy vehicles of the Harmonoise model, respectively. The light vehicle in the ASJ model is associated with the light vehicle in the Harmonoise model. Under the association, three steps marked as (a)–(c) in Figure 2 are added to the calculation procedure of the Harmonoise model to obtain consistent quantities with the ASJ model. Step (a) calculates the single-vehicle A-weighted power level for all subsources in source point i, $L_{W\mathrm{A,HN},i}$ (HN stands for the Harmonoise model hereafter), by incoherent summation of $L'_{W,i,hs}$ over all subsources and all bands with the A-weights applied. The $L_{W\mathrm{A,HN},i}$ is considered to be comparable with $L_{W\mathrm{A},i}$ of the ASJ Model. Step (b) calculates the A-weighted source directivity, C_{dirA} as

$$C_{\mathrm{dirA}} = L'_{WA,\mathrm{dir}} - L'_{WA} \tag{3}$$

where $L'_{WA,\mathrm{dir}}$ is the A-weighted incoherent summation of all bands and all subsources of $L'_{W,i,hs}$ with the source directivity C_{dir} applied, and L'_{WA} is the same but without application of the source directivity. In calculating C_{dirA}, directivity angles defined by the ASJ and the Harmonoise models, (ϕ_{A}, θ) and (Ψ, ϕ_{H}) shown in Figure 3, respectively, are associated with the help of an auxiliary variable Θ by

$$\phi_{\mathrm{A}} = \tan^{-1}\left[(\cos\Theta)/(\tan\Psi)\right], \tag{4}$$

$$\theta = \tan^{-1}\left(\sin\phi_{\mathrm{A}}\tan\Theta\right) \quad (\phi_{\mathrm{A}} \neq 0), \tag{5}$$

$$\Theta = 90^{\circ} - \phi_{\mathrm{H}}. \tag{6}$$

The C_{dirA} is considered to be comparable with ΔL_{dir} of the ASJ model. Step (c) calculates the A-weighted single-vehicle SPL for all subsources in source point i, $L_{\mathrm{A,HN},i}$. For this, the one-third-octave-band SPL for a single-vehicle subsource, $L_{\mathrm{HN},i,hs}$ is calculated by

$$L_{\mathrm{HN},i,hs} = L'_{W,i,hs} - \Delta A_{\mathrm{H},i,hs} \tag{7}$$

Then, $L_{\mathrm{A,HN},i}$, is obtained by incoherent summation of $L_{\mathrm{HN},i,hs}$ over all subsources and all bands with the A-weights applied. The $L_{\mathrm{A,HN},i}$ is considered to be comparable with $L_{\mathrm{A},i}$ of the ASJ model.

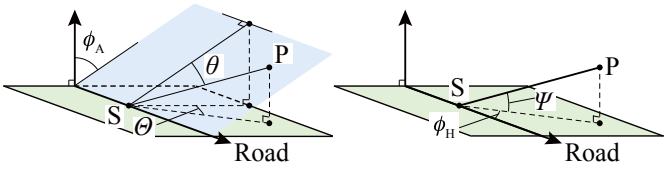

(a) ASJ RTN-Model 2013 (b) Harmonoise

Figure 3 – Definitions of the directivity angles in the ASJ and the Harmonoise models. S and P are the source and the receiver, respectively

3. NUMERICAL EXPERIMENTS

3.1 Test Cases

Cases 01 and 05 included in a collection of Harmonoise test cases (12) are used in this study. The configurations of Cases 01 and 05 are a straight road in a semi-free field as shown in Figure 4, and a thick barrier along a straight road as shown in Figure 5, respectively. Case 05 has two patterns of barriers heights h_{b} = 8 m and 15 m. The patterns are called Maps 11 and 12, respectively. In both cases, the source road with a length of 2 000 m is placed along y-axis. The source road has Lanes 1 and 2 with a 10 m interval and with vehicles running towards the negative and positive direction of the y-axis, respectively. Receiver P is placed at a height of 4 m with a horizontal distance of 55 m from Lane 1 of the source road. Each lane has 501 source positions with a uniform interval of 4 m. Parameter settings are shown in Tables 2 and 3. Meteorological effect is not taken into account.

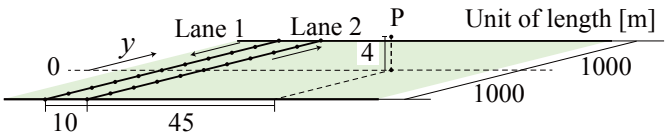

Figure 4 – Geometry of Case 01: Semi-free field

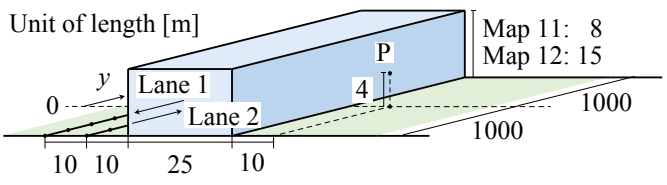

Figure 5 – Geometry of Case 05: Screening by thick barriers

Table 2 – Calculation settings (1)

Road surface	DAC 0/11
Representative flow resistivity [kNs/m^4]	20 000
Air temperature [℃]	15

Table 3 – Calculation settings (2)

Vehicle type	ASJ	Large-sized	Medium-sized	Light
	Harmonoise	Heavy	Medium heavy	Light
Vehicle speed [km/h]		50		
Traffic flow [/h]		50	100	3 000
Temperature coefficient [dB/°C]		0.05	0.05	0.10

The insertion loss by the thick barrier for the ASJ model $\Delta L_{\mathrm{IL,ASJ},i}$ and for the Harmonoise model $\Delta L_{\mathrm{IL,HN},i}$ are calculated from $L_{\mathrm{A},i}$ and $L_{\mathrm{A,HN},i}$, respectively, for Cases 01 and 05, $L_{\mathrm{A,ASJ},i,\mathrm{free}}$, $L_{\mathrm{A,ASJ},i,\mathrm{barrier}}$, $L_{\mathrm{A,HN},i,\mathrm{free}}$ and $L_{\mathrm{A,HN},i,\mathrm{barrier}}$ as

$$\Delta L_{\mathrm{IL,ASJ},i} = L_{\mathrm{A,ASJ},i,\mathrm{barrier}} - L_{\mathrm{A,ASJ},i,\mathrm{free}}, \tag{8}$$

$$\Delta L_{\mathrm{IL,HN},i} = L_{\mathrm{A,HN},i,\mathrm{barrier}} - L_{\mathrm{A,HN},i,\mathrm{free}} \tag{9}$$

3.2 Finite-Difference Time-Domain Simulations

To obtain reference solutions, three-dimensional finite-difference time-domain (FDTD) simulations are carried out. Figure 6 shows the configuration. Only regions around y = 0 [m] in Figures 4 and 5 are solved, otherwise computational cost becomes too much. Thus the configuration only contains a single point source for y = 0 [m], S_1, which is simulated by a Gaussian initial distribution of the pressure. The size of (h, h_b) in Figure 6 are (4.5, 0) m, (11, 8) m and (18, 15) m for Case 01, Case 05 Map 11 and Map 12, respectively. Other computational parameters are listed in Table 4. The A-weighted SPL $L_{\mathrm{A,ref},i}$ is computed from the one-third-octave-band spectrum of the solution with the inverse spectrum of the initial Gaussian sound source, the power spectrum of the source vehicle and the A-weights applied. The frequency range is limited from 50 Hz to 2.5 kHz because of the computational grid size. The insertion loss by the thick barrier, $\Delta L_{\mathrm{IL,ref},i}$, is calculated from $L_{\mathrm{A,ref},i}$ for Cases 01 and 05, $L_{\mathrm{A,ref},i,\mathrm{free}}$ and $L_{\mathrm{A,ref},i,\mathrm{barrier}}$, respectively, as

$$\Delta L_{\mathrm{IL,ref},,i} = L_{\mathrm{A,ref},i,\mathrm{barrier}} - L_{\mathrm{A,ref},i,\mathrm{free}} \tag{10}$$

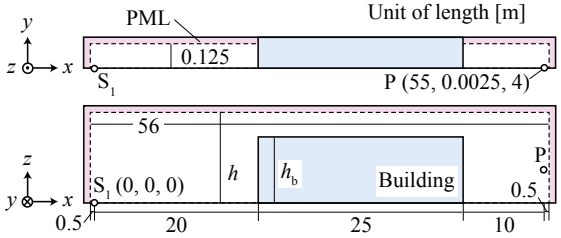

Figure 6 – Configuration of the FDTD simulations. The y and other axes are not to scale

Table 4 – Computational parameters and values

Parameter	Value
Grid size [m]	5×10^{-3}
Time step [s]	8×10^{-6}
Number of steps	31 250
Half width at half maximum of sound source [m]	2.5×10^{-3}
Speed of sound [m/s]	340
z-coordinates of the source [m]	0, 0.3, 0.75
Density of air [kg/m^3]	1.205

4. RESULTS

Hereafter, a large-sized vehicle of the ASJ model and a heavy vehicle of the Harmonoise model

are collectively called a heavy vehicle.

4.1 Source Power Levels

Figure 7 shows ΔL_{dir} and C_{dirA} for each vehicle category. For heavy vehicles, the power level of the ASJ model reduces as Ψ increases and is symmetrical to $\Theta = 0°$. The power level of the Harmonoise also reduces as Ψ increases, but is asymmetric to $\phi_{\mathrm{H}} = 90°$ and is stronger for the forward direction. For light vehicles, the directivity is similar for both models in that the power level reduces as Ψ increases and is symmetrical to $\Theta = 0°$ and $\phi_{\mathrm{H}} = 90°$.

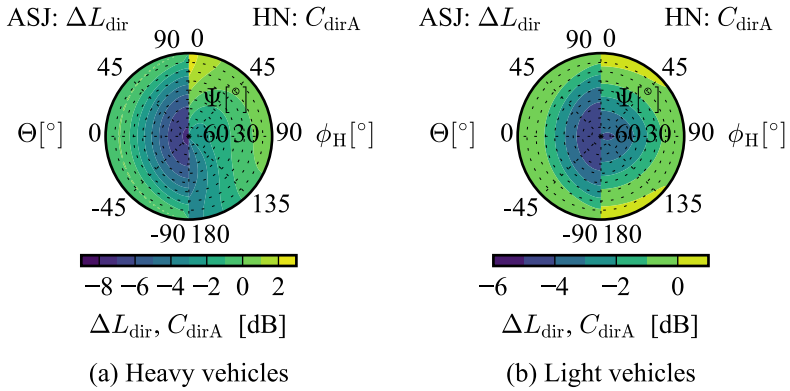

Figure 7 – Source directivity of a (a) heavy and (b) light vehicle of the ASJ and Harmonoise (HN) models

The A-weighted source power level without the source directivity taken into account is shown in Figure 8. The power levels for the heavy vehicles are nearly identical between the models, whereas that for the light vehicle of the ASJ model is larger by 2 dB than the Harmonoise model.

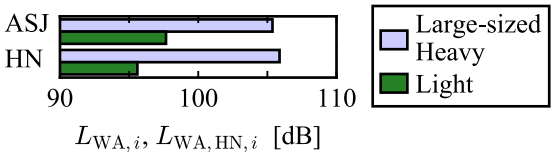

Figure 8 – A-weighted source power level without source directivity taken into account

4.2 Insertion Loss and A-weighted SPL

The results presented here except for the final L_{Aeq} are those for Lane 1 because those for both lanes are similar. The calculation of L_{Aeq} uses the results for both lanes.

Figure 9 presents the insertion losses with respect to the source at $y = 0$ without the source directivity taken into account in comparison with the reference solutions. The difference between the model calculations and the reference solutions are less than 1 dB for Map 11 and approximately 3 dB for Map 12. Although slightly larger difference with deeper diffraction by the barriers is seen for both models, the difference for each case is nearly identical between the models and relatively small.

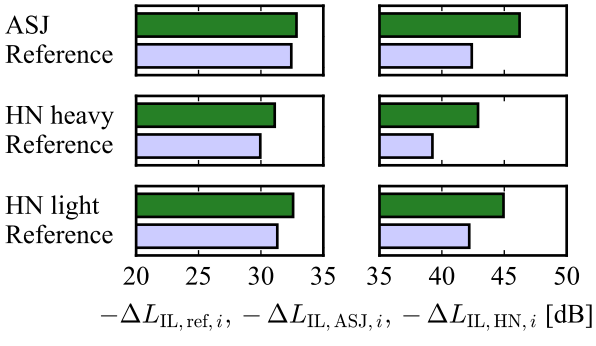

(a) Case 05: Map 11 (b) Case 05: Map 12

Figure 9 – Insertion losses for Case 05 (a) Map 11 and (b) Map 12 without the source directivity

Figure 10(A) plots $L_{A,i}$ and $L_{A,HN,i}$ as functions of the y-coordinate of source i for Case 01, Case 05 Map 11 and Map 12 without the source directivity taken into account. The plots can be regarded as simulated single-vehicle pass-by patterns (the unit patterns) observed at the receiver. For all cases the plots are symmetrical to $y = 0$ [m]. For Case 01, a clear geometric attenuation pattern is observed towards the left and the right ends. For Case 05 Maps 01 and 12, the pattern is not so clear as the geometric attenuation and the diffraction attenuation cancel each other. Figure 10(B) similarly plots $L_{A,i}$ and $L_{A,HN,i}$ with the source directivity taken into account. The plots for the heavy vehicle of the Harmonoise model for all cases are characteristic in that they are asymmetrical to $y = 0$ [m] as expected from the source directivity shown in Figure 7(a). The $L_{A,i}$ for the large-sized vehicle of the ASJ model at $y = 0$ [m] indicated by the (I) label in Figure 10(B) is 2.3 dB smaller than that in Figure 10(A). This is because the source power is lost by the application of the source directivity. The plots for the light vehicles are similar to those for the heavy vehicles.

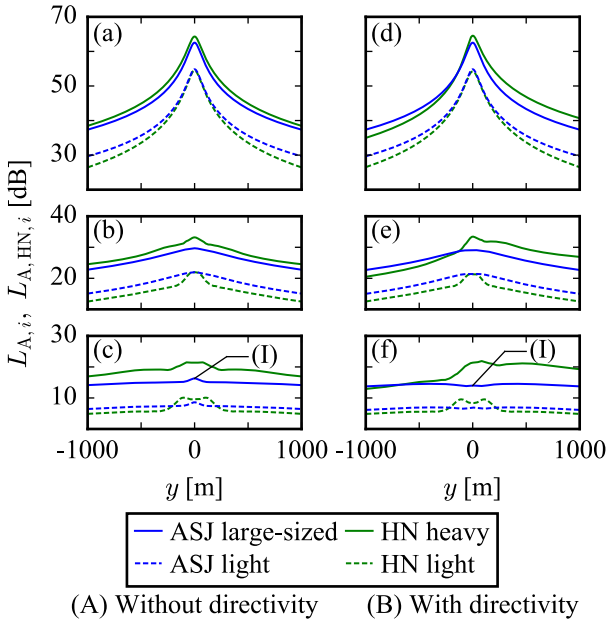

Figure 10 – $L_{A,i}$ and $L_{A,HN,i}$ for (a), (d) Case 01, (b), (e) Case 05 Map 11, (c), (f) Case 05 Map 12

In all cases plotted in Figure 10, for heavy vehicles the SPLs for the Harmonoise model is larger than those for the ASJ model. This is because the insertion loss is smaller for the Harmonoise model as illustrated in Figure 9 whereas the source power levels are nearly identical as indicated in Figure 8. For light vehicles, the SPL of the ASJ model is generally larger for Case 05 map 11. This is because the source power level is larger for the ASJ model as illustrated in Figure 8 whereas the insertion loss is nearly identical as illustrated in Figure 9. On the other hand, for Case 05 Map 12 the SPL for the ASJ model is generally smaller around $y = 0$ [m]. This is because the insertion loss of the ASJ model is larger than the Harmonoise model.

Figure 11 shows L_{Aeq} for each case without and with the source directivity taken into account. When the source directivity is not taken into account, the L_{Aeq} are nearly identical between both models for Case 01. For Case 05, the L_{Aeq} of the ASJ model is larger for Map 11 but smaller for Map 12 than the Harmonoise model. This follows the observation of light vehicles in Figure 10 as the light vehicles mostly occupy the traffic volume, as shown in Table 3. The difference between without and with the source directivity becomes larger as the height of the barrier becomes larger. In all cases, differences between the models are less than 2 dB.

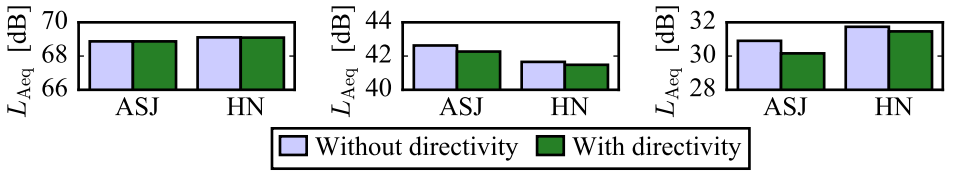

(a) Case 01 (b) Case 05: Map 11 (c) Case 05: Map 12

Figure 11 – L_{Aeq} for (a) Case 01, Case 05 (b) Map 11 and (c) Map 12

5. CONCLUSIONS

In this study, a methodology to derive consistent quantities between the ASJ model and the European Harmonoise model is established. The methodology is applied to thick barrier test cases that are included in a Harmonoise deliverable. At the same time, finite-difference time-domain simulations are carried out to obtain reference solutions. A-weighted source power levels between the two models are found to be larger for the light vehicle of the ASJ model. Comparison between each model and the reference solutions weighted by each source spectrum agree well for both models. Single-vehicle pass-by patterns of the Harmonoise model become asymmetrical to $y = 0$ [m] when the source directivity is taken into account. The final A-weighted levels obtained by both models agree within a 2 dB difference. However, the difference in the source directivity and the balance of the source power level and the diffraction attenuation may lead to large difference under certain cases.

ACKNOWLEDGEMENTS

This work was supported by JSPS KAKENHI 16H04462, 17H03350, 18K18897, Grant-in-Aid for JSPS Fellows 19J13172 and a grant-in-aid contract with The Niigata Engineering Promotion, Inc.

REFERENCES

1. Kragh J, Plovsing B, Storeheier S, Taraldsen G, Jonasson H, Saarinen A. Nord2000. Comprehensive outdoor sound propagation model. Part 1: Propagation in an atmosphere without significant refraction. Report AV 1849/00. Hørsholm, Denmark: Delta; 2006. p. 1-127.
2. Nota R, Barelds R, Maercke D. Harmonoise WP 3 engineering method for road traffic and railway noise after validation and fine tuning. Technical Report HAR32TR-040922-DGMR20. Arnhem, The Netherlands: DGMR; 2005. p. 1-E-21.
3. Kephalopoulos S, Paviotti M, Anfosso-Lédée F. Common noise assessment methods in Europe (CNOSSOS-EU). EUR 25379 EN. Luxembourg, Luxembourg: Publications Office of the European Union; 2012. p. 1-180.
4. Steele C. A critical review of some traffic noise prediction models. Appl Acoust. 2001;62(3):271–287.
5. Garg N, Maji S. A critical review of principal traffic noise models: Strategies and implications. Environ Impact Assess Rev. 2014;46:68-81.
6. Jónsson G, Jacobsen F. A comparison of two engineering models for outdoor sound propagation: Harmonoise and Nord2000. Acta Acust United Acust. 2008;94:282-289.
7. Maercke D, Salomons E. The Harmonoise sound propagation model: further developments and comparison with other models. Proc NAG/DAGA 2009 Int Conf; 23-26 March 2009; Rotterdam, The Netherlands 2009. p. 1622-1625.
8. Ecotiere D, Foy C, Dutilleux G. Comparison of engineering models of outdoor sound propagation: NMPB2008 and Harmonoise-Imagine. Proc Acoust 2012 Nantes Conf; 23-27 April 2012; Nantes, France 2012. p. 1523–1527.
9. Kokkonen J. CNOSSOS-EU noise model implementation in Finland and experience of it in 3rd END round. Proc Euronoise 2018; 27-31 May 2018; Crete, Greece 2018. p. 1219-1224.
10. Sakamoto S. Road traffic noise prediction model "ASJ RTN-Model 2013": Report of the Research Committee on Road Traffic Noise. Acost Sci Technol. 2015;36:49-108.
11. Maercke DV. Programing the Point-to-point Propagation Model. Technical Report HAR34TR-041124-CSTB01. Marne-la-Vallée, France: CSTB; 2004. p. 1–77.
12. Nota R. Performance of the Harmonoise WP 3 Engineering method in urban situations - test cases. Technical Report HAR35TR-050111-DGMR10. Arnhem, the Netherlands: DGMR; 2005. p. E-2-E-21.